14. Jobling, S. A. and Gehrke, L., Enhanced translation of chimaeric messenger RNAs containing viral untranslated leader sequence. *Nature*, 1987, **325**, 622–625.
15. Kozak M., Compilation and analysis of sequences upstream from the translation start site in eukaryotic mRNAs. *Nucleic Acids Res*., 1984, **12**, 857–872.
16. Hajdukiewicz, P., Svab, Z. and Maliga, P., The small versatile *pPZP* family of *Agrobacterium* binary vectors for plant transformation. *Plant Mol. Biol*., 1994, **25**, 989–994.
17. Mattanovich, D., Ruker, F., Machado, A., Laimer, M., Regner, F., Steinkellner, H., Himmler, G. and Katinger, H., Efficient transformation of *Agrobacterium* spp. by electroporation. *Nucleic Acids Res*., 1989, **17**, 6747.
18. Rogers, S. O. and Bendich, A. J., Extraction of total cellular DNA from plants, algae and fungi. In *Plant Molecular Biology Manual* (eds Gelvin, S. B. and Schilperoort, R. A.), Kluwer, Dordrecht, 1994, pp. 1–8.
19. Klimyuk, V. I., Carroll, B. J., Thomas, C. M. and Jones, J. D. G., Alkali treatment for rapid preparation of plant material for reliable PCR analysis. *Plant J*., 1993, **3**, 493–494.
20. Dale, E. C. and Ow, D. W., Gene transfer with subsequent removal of the selection gene from the host genome. *Proc. Natl. Acad. Sci. USA*, 1991, **88**, 10558–10562.

ACKNOWLEDGEMENTS. This work was supported by a research grant from the National Dairy Development Board and its subsidiary DOFCO and the Department of Biotechnology, New Delhi. NCB was supported by a Research Fellowship from the Council of Scientific and Industrial Research (CSIR), India. We thank A. K. Pradhan, Anil Grover and Arun Jagannath for support with materials and helpful discussions.

Received 21 February 2004; revised accepted 24 June 2004

Validation of multi-channel scanning microwave radiometer on-board Oceansat-I

P. M. Muraleedharan[1,*], T. Pankajakshan[1] and M. Harikrishnan[2]

[1]National Institute of Oceanography, Goa 403 004, India
[2]National Institute of Ocean Technology, Chennai 601 302, India

Sea surface temperature (SST), sea surface wind speed (WS) and columnar water vapour (WV) derived from Multi-frequency Scanning Microwave Radiometer (MSMR) sensor on-board IRS-P4 (Oceansat-I) were validated against the *in situ* measurements from ship, moored buoy (MB), drifting buoy (DB) and autonomous weather station (AWS). About 1400 satellite *in situ* match-ups were used for the validation of SST and WS, while only 60 match-ups were available for the validation of WV. Therefore specific humidity, Q_a was used as a proxy for validating WV.

The drifting buoy SSTs showed good correlation with the satellite values ($r = 0.84$). The correlation of MB SSTs was better during night when the WS varied between 0 and 10 m/s. During the day, correlation peaked for higher wind speeds (> 10 m/s). MB ($r > 0.80$) was relatively better than AWS ($r \sim 0.70$) and ship ($r < 0.50$) for validating satellite-derived WS. Daytime winds exhibited better correlation with satellite values when measured from ocean platforms (MB and ship), but the winds measured from land-based platforms (AWS) were closer to satellite values during night-time. Q_a values consistently showed higher correlation with satellite values during night-time. The low root mean square deviation (RMSD) of DB SST (1.17°C) and MB WS (1.52 m s^{-1}) is within the achievable accuracy of the microwave sensor when validated with data collected over the tropical Indian Ocean. The RMSD of Q_a (1.81 g kg^{-1}), however, falls much beyond the attainable accuracy of the microwave sensor.

IRS-P4 (Oceansat-I) launched on 26 May 1999 carried an all-weather capable Multi-frequency Scanning Microwave Radiometer (MSMR) payload besides Ocean Colour Monitor (OCM). Details of these payloads are described elsewhere[1]. Channels of MSMR are suitable to retrieve sea surface temperature (SST), sea surface wind speed (WS), columnar water vapour (WV) and cloud liquid water on a global scale. The 6.6 GHz band, suitable for the retrieval of SST and WS (along with 10 GHz), was an improvement over the contemporary sensors (SSM/I, SSMR, etc.).

Weak microwave radiation in these channels makes the spatial resolution more coarse, but is still useful for supplementing high-resolution, cloud-sensitive AVHRR data[2]. Microwave radiometers can measure SST with an accuracy[3,4] of ± 1.5°C, which is much coarser than the one (± 0.5°C) attainable from thermal infrared sensors[5]. Wentz *et al.*[6] showed that passive microwave radiometers can measure WS with an accuracy of approximately 2 m s^{-1}, which is as good as the scatterometer and altimeter-derived WS. Retrieval accuracy of WV from Nimbus 5 microwave spectrometer was shown[7] to be 0.2 g cm^{-2} and it improved substantially to 0.07 g cm^{-2} when derived from SSM/I on-board DMSP satellite[8].

The objectives of this satellite validation exercise are to (a) identify the best frequency combinations to derive SST, WS and WV from satellite sensors by comparing with *in situ* data, (b) identify suitable *in situ* platform for validating satellite-derived SST, WS and WV, (c) study the role of WS in the satellite SST validation and (d) understand the accuracy of MSMR measurements.

The MSMR geophysical data product supplied by the National Remote Sensing Agency consists of 24 h data and has been generated on three different grid sizes, viz. 150 km (grid I), 75 km (grid II) and 50 km (grid III). Details of the grids are given elsewhere[1].

The sea truth data for SST, WS and WV were collected for two years from sensors mounted on various platforms

*For correspondence. (e-mail: murali@darya.nio.org)

deployed over the tropical Indian Ocean, immediately after the launch of the satellite (Figure 1). SSTs were measured from ship, drifting buoy (DB) and moored buoy (MB), while WS was measured from ship, MB and autonomous weather station (AWS) (installed in the coral island of Kavarathi). WV values measured from *in situ* platforms were few in number compared with SST and WS. The validation of WV was therefore carried out by estimating specific humidity (Q_a) from satellite data (WV) following Liu[9]. An equivalent *in situ* Q_a was then computed from the surface met parameters.

Time variation of SST (MB) and WS (MB and AWS) was subjected to autocorrelation analysis. The drop in autocorrelation coefficient for SST was marginal even over a 24 h time window, while it deteriorated fast for WS after 3 h (Table 1). Hence in the present analysis all MSMR observations falling within the time interval of 2 h or less with respect to *in situ* measurements have been considered as coincident. The spatial distribution of the standard deviation of each of the MSMR parameters with different windows (viz. 2° × 2°, 3° × 3° boxes) suggests that these standard deviations are well within the pre-launch projected accuracy of each of these parameters[10]. Hence in the present validation experiment, a maximum search radius of 2° has been considered.

Details of synchronized data (weighted average of satellite values against *in situ* observation) obtained during the validation period are given Table 2. Day and night match-ups are separated for studying the nature of the diurnal relationship. Spurious MSMR values were discarded to safeguard the relationship by following a simple scheme of analysis. The collocated datasets of both SST and WS were subjected to this scheme of analysis. The correlation coefficients were calculated for each set of SST/WS data. The correlation improves for both cases when the scatter was reduced. An *X*–*Y* plot between cor-

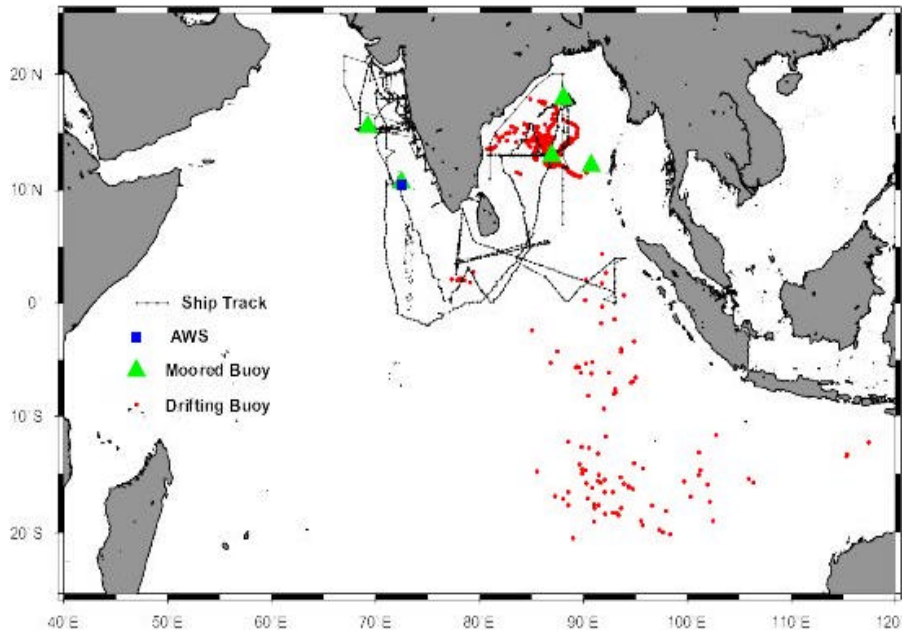

Figure 1. *In situ* platforms used for the validation experiment.

Table 1. Autocorrelation analysis of SST and WS from MB (DS1, DS2, DS3) and WS from AWS

Time lag (h)	DS1 (15.5°N; 69.2°E) *n* = 1451		DS2 (10.5°N; 72.5°E) *n* = 1197		DS3 (12.2°N; 90.7°E) *n* = 436		AWS (10.5°N; 72.0°E) *n* = 933
	r of SST	*r* of WS	*r* of SST	*r* of WS	*r* of SST	*r* of WS	*r* of WS
03	0.98	0.79	0.98	0.88	0.97	0.68	0.86
06	0.96	0.62	0.97	0.81	0.94	0.58	0.81
09	0.95	0.53	0.96	0.77	0.92	0.44	0.78
12	0.95	0.48	0.95	0.74	0.91	0.42	0.76
15	0.95	0.47	0.95	0.74	0.90	0.39	0.74
18	0.95	0.48	0.96	0.75	0.89	0.37	0.74
21	0.96	0.50	0.97	0.76	0.90	0.35	0.73
24	0.97	0.49	0.97	0.77	0.88	0.32	0.72

relation coefficient (r) and the sea truth–MSMR difference discarded is shown in Figure 2 *a*. Figure 2 *b* illustrates the relationship between percentage of data lost and the sea truth–MSMR difference discarded. The value of r is highest for SST/WS when the sea truth–MSMR difference is brought to a minimum (1°C or 1 m s^{-1}), but the data lost are 90%, which is definitely unscientific. The correlation coefficient decreases as the discarded sea truth–MSMR gap widens. Three-degree cut-off limit in SST data yields a correlation coefficient of 0.40 (Figure 2 *a*) allowing a data loss of 20% (Figure 2 *b*). The relationship is statistically significant with this value of r when it represents 80% of the samples. The corresponding cut-off limit for WS is 7 m/s to sustain a statistically significant correlation coefficient of 0.65 (Figure 2 *a*). Here, the sea truth–MSMR difference higher than 7 m/s accounted for less than about 20% of the total sample (Figure 2 *b*). In short, in the present validation exercise, the collocated dataset for SST represented only those MSMR values which were close to the ground truth by ± 3°C. The remaining values higher than this cut-off limit were discarded. Similarly the cut-off limit for WS was 7 m/s.

The negative bias indicated colder satellite SST (against DB-SST) and its removal reduced the *y*-intercept and brought fit closer to the origin (Figure 3 *a*). On the contrary, the positive bias of ship-SST (Figure 3 *b*) and MB-SST (Figure 3 *c*) (warmer satellite SST) retained the *y*-intercept even after the removal of bias. Temperature of the surface thin layer (few mm thick) picked up by the satellite was closer (r = 0.84) to the DB-SST measured at 20 cm depth. The uneven sensor accuracies of DBs generated systematic bias with satellite data and their removal reduced the *y*-intercept (Figure 3 *a*). Bulk temperature of the surface 2–3 m layer measured by ship and MB were compared with skin-SST derived by satellite. The diurnal temperature disparity between these two depths was the cause of random error, which compounded by human error factor that is more prevalent in ship measurement. The random error retains the *y*-intercept even after bias removal (Figure 3 *b* and *c*). Therefore, DB becomes the natural choice while selecting platforms for validating satellite-derived SST.

The effect of wind on SST validation was examined for various WS ranges (e.g. 1–5, 5–10 and 10–15 m/s) using data from MB deployed over central Arabian sea and Bay of Bengal. The day–night values were separately subjected to this analysis for various spatial and temporal windows to study the nature of the relationship. The nighttime SSTs exhibited better relationship when the WS was lower than 10 m/s (Figure 4). The satellite measures the

Table 2. Details of *in situ* platforms, period of observation and collocated datapoints. Day and night match-ups are displayed separately

Platform	Parameter	Period	No. of match-ups obtained		
			Day	Night	Both
Ship	SST	18 cruises (1999–2001)	94	84	178
	WS	–do–	59	70	129
DB	SST	10–14 ARGO drifters from June 1999 to September 2001	207	266	473
MB	SST	June 1999 to February 2001	490	451	941
	WS	–do–	488	574	1062
AWS	WS	April 2000 to September 2001	420	490	910

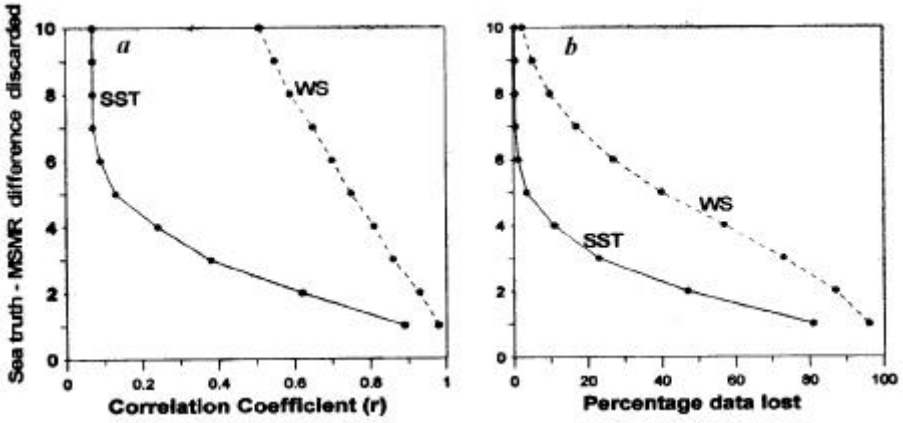

Figure 2. Correlation coefficient between satellite and sea-truth values when the scatter higher than various thresholds is discarded (***a***) and percentage of the data lost when the scatter higher than various thresholds is discarded (***b***).

temperature of the thin surface layer as it contributes more to the emissivity[2,3], whereas the MB measurements represent the surface 2–3 m layer. Diurnal variation of air temperature will instantly modify the temperature of the surface layer immediately in contact with the atmosphere, which will in turn modify the emissivity and thus the satellite values[11]. During daytime, the thin top layer of the ocean gets heated and expands, which ultimately leads to stratification. The satellite often records the temperature of this upper stratified layer. This surface temperature (of the stratified layer) is not necessarily picked up by platforms like the MB which measures only the bulk SST representing the surface 2–3 m layer. Therefore, this mixed layer temperature need not match with that of the surface stratified layer that the satellite measures. So the relationship (r) tends to decrease. On the contrary, during night-time the top thin layer of the ocean cools and supports convection and subsequent mixing. This mixed layer temperature is recorded by platforms like the MB. So both satellite and MB measure temperatures of the same mixed-layer during night-time. The relationship (r) thus tends to increase. This is true so long as the wind does not interfere with the surface processes. Surface mixing is often associated with high WS (> 10 m s^{-1}) that ultimately destroys the surface-layer stratification during daytime, enabling the satellite and MB to pick up the same mixed

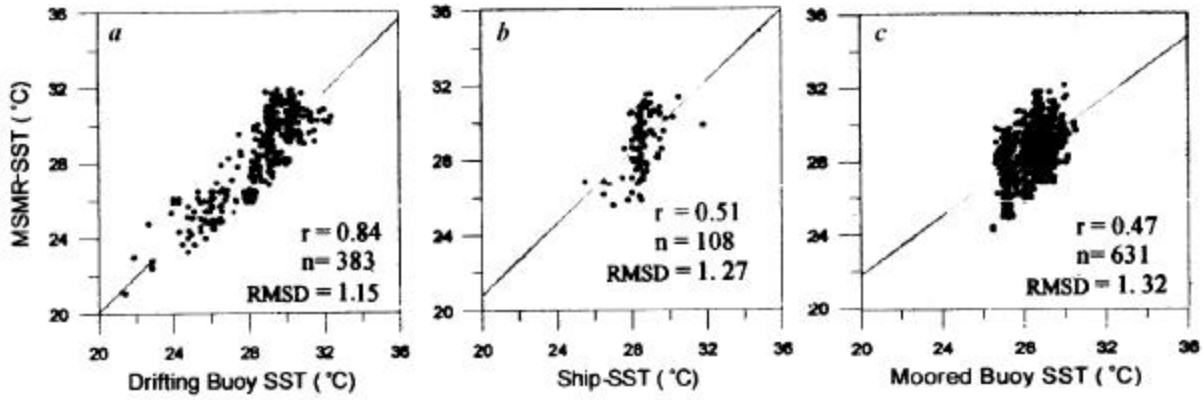

Figure 3. MSMR-SST vs DB-SST (***a***), ship-SST (***b***) and MB-SST (***c***) (after bias removal) in the spatial and temporal windows of 1° × 1°latitude–longitude grid and 120 min respectively.

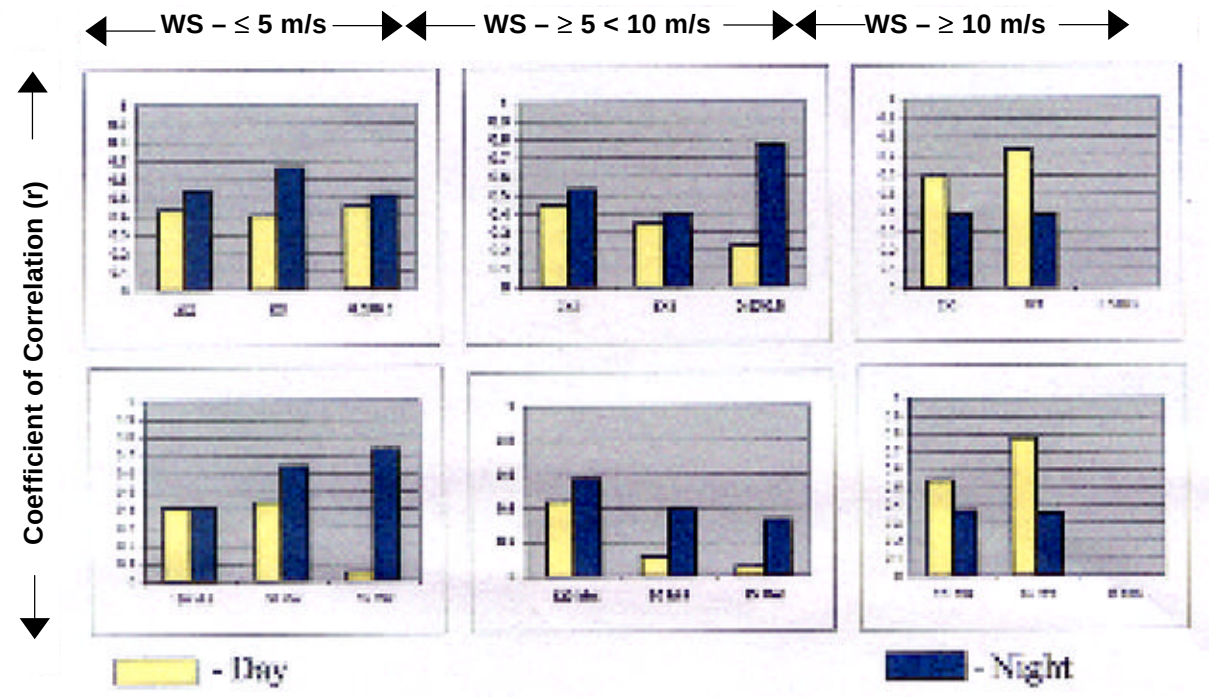

Figure 4. Day and night correlation between satellite and sea-truth-based SSTs for various wind conditions. Spatial and temporal grids are illustrated in the top and bottom panels respectively.

layer temperature. This leads to a better correlation during daytime when the winds are strong. Although mixing due to high WS does occurs at night, both satellite and MB measure the subdued mixed-layer temperature. Satellite–sea-truth relationship appears to improve for higher temperature (daytime) and tends to degrade for lower temperature (night-time) when the WS is higher than 10 ms^{-1}.

MSMR retrieves WS in two modes, viz. grid1 (150 km × 150 km) and grid2 (75 km × 75 km). The relatively high RMSD and low correlation make the grid2 product less important (details not given). The scatter plots in Figure 5 highlight the worthiness of MB ($r = 0.81$) in validating the MSMR data. Initially, MB and AWS exhibited large positive bias (> 3 m/s) compared to ship (> 1 m/s), but its removal reduced the root mean square deviation (RMSD) considerably for both MB and AWS and the decrease was marginal for ship (details not shown). As the inter-calibration of sensors was not meticulously followed during this validation period, bias due to systematic error has crept into the observation. The disappearance of *y*-intercept is an indication of the removal systematic bias in Figure 5 *a* and *c*. The ship-based wind measurement, however, has the disadvantage of its structure interfering with the wind pattern. The error due to the modified wind pattern was compounded by human error in measuring WS. This contributes to random error that retained the *y*-intercept even after the removal of bias (Figure 5 *b*).

The correlation (r) was higher during both day and night for stationary platforms like MB and AWS, while it deteriorated for moving platforms (ship; Figure 6). This could be attributed to the error arising from the influence of the built-in structure of the vessel in modifying the WS. WS measured from ocean platforms (MB and ship) during day time was closer to the satellite measurement, but the night wind gave better correlation when measured from the island-based weather station (AWS). A proper explanation to this discrepancy is yet to be evolved. Land contamination of the radiation received at the satellite due to the presence of a small piece of land in the fairly big field-of-view of the microwave sensor cannot be ruled out completely and its ability in modifying the radiation to affect the day–night discrepancy is worth studying.

MSMR measures WV in three modes (grid1, grid2 and grid3). Due to the lack of synchronized upper air observations, an indirect method was adopted to validate this parameter. The surface-level specific humidity Q_a was computed from both satellite and sea-truth values. A fifth degree polynominal expression[9] was used to compute Q_a from satellite-derived total WV data with an inherent accuracy[8] of 2.2 g kg^{-1}. This amounts to an uncertainity of 10–15%. The Q_a value was compared with those values computed from wet bulb–dry bulb combinations in the case of Ship data and from relative humidity–air temperature combinations in the case of AWS data. The uncertainty in estimating Q_a from surface met parameters could be roughly estimated[12] to 10–15%. Computation of Q_a from both satellite and *in situ* data yielded the same amount of uncertainty (10–15%). This justifies the exercise of using Q_a as proxy for validating WV derived from MSMR.

The sea truth–satellite relationship indicated that the grid1 data product has a marginal edge over the grid2 and grid3 products (details not presented here). RMSD between satellite and *in situ* (ship and AWS) Q_a values came down drastically during daytime followed by an increase in r (> 80%; Figure 7 *a* and *c*). But the relationship deteriorated during night for ship (high RMSD and low r; Figure 7 *b*). The marginal diurnal variation of the sea truth–satellite relationship (Figure 7 *d*) makes AWS a better choice for validating the proxy parameter Q_a.

The day–night contrast in correlation between satellite and *in situ* platform is unambiguously displayed in Figure 8 for both AWS and ship. Diurnal contrast in correlation was consistent irrespective of platforms and space–time windows. Atmospheric humidity is high during daytime as the evaporation peaks during these hours. Moisture-sensitive microwave channels pick up this enhanced

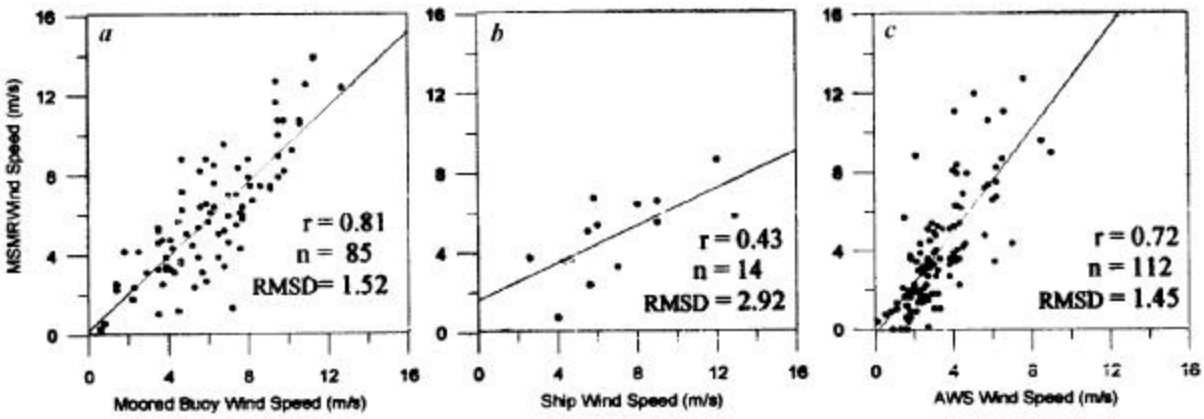

Figure 5. MSMR-WS vs MB-WS (***a***) ship-WS (***b***) and AWS-WS (***c***) (after bias removal) in the spatial and temporal windows of 0.5° × 0.5º latitude–longitude grid and 60 min respectively.

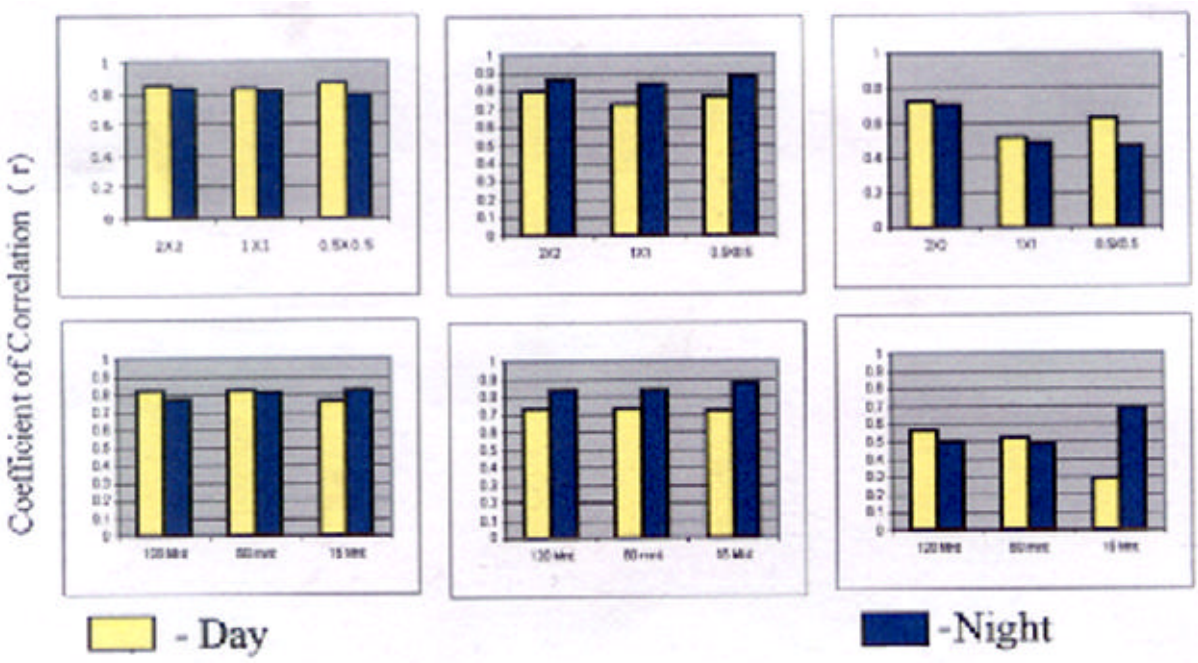

Figure 6. Coefficient of correlation of WS between satellite and sea-truth measurements [MB (left panel), AWS (middle panel) and ship (right panel)] in spatial (top panel) and temporal (bottom panel) grids.

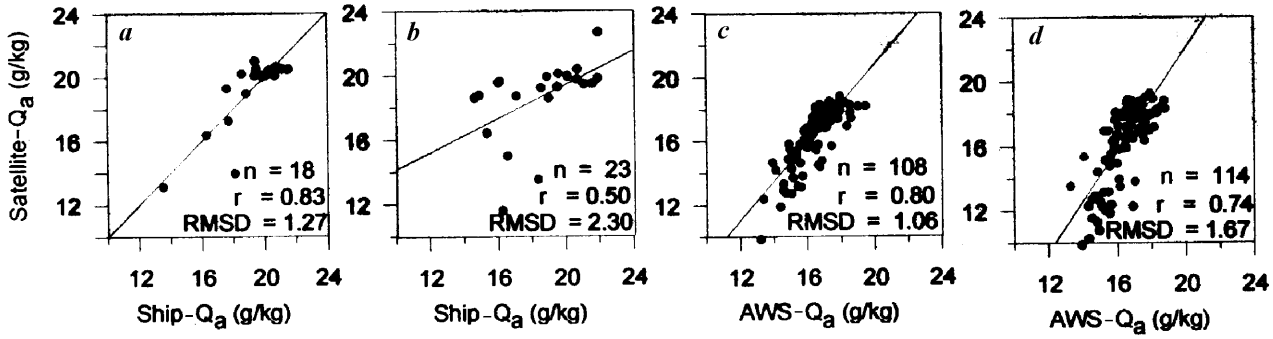

Figure 7. MSMR Q_a vs Ship Q_a during day (***a***) and night (***b***) hours. Similar relationships for AWS are displayed in (***c***) and (***d***). Biases were removed in all cases.

absorption signal with greater accuracy during daytime. Subdued night-time absorption signals reduce the accuracy of the retrieval, which probably gives rise to the day–night contrast in the relationship.

The attainable accuracy (global) of present microwave sensors for retrieving SST[4], WS[6] and WV[7] is 1.5°C, 2 m s^{-1} and 0.2 g cm^{-2} respectively. WV retrieval accuracy of 0.2 g cm^{-2} is equivalent to an RMS error of 0.77 g kg^{-1} of specific humidity Q_a. Direct retrieval of Q_a from MSMR brightness temperature data also produced an RMS error of 0.84 g kg^{-1} in monthly timescale[13]. Validation of MSMR was carried out using *in situ* data collected over the tropical Indian Ocean and hence the accuracies obtained are region-specific. Platforms for validating MSMR parameters were identified and listed with error statistics in Table 3. The RMSD (after bias removal) of MSMR sensors in retrieving SST, WS and Q_a (proxy for WV) over tropical Indian Ocean are 1.15°C, 1.52 m s^{-1} and 1.81 g kg^{-1} respectively. The low RMSD of SST and WS is within the achievable accuracy of the microwave sensor. The RMSD of Q_a however, falls much beyond the attainable accuracy when validated with data collected over the tropical Indian Ocean.

Satellite-derived grid1 geophysical data products are closer to the sea-truth values for SST, WS and WV. DB, MB and AWS are suitable platforms for validating SST, WS and Q_a (proxy for WV) respectively. Satellite SST values were closer to sea-truth during night hours, when the WS varied from 0 to 10 m/s. The same relationships hold good during daytime when the WS was higher than

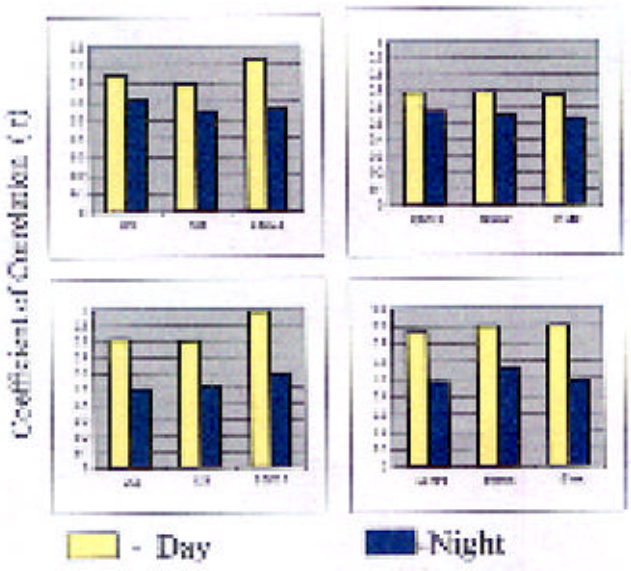

Figure 8. Day and night correlation of Q_a between satellite and sea-truth [AWS – top panel; ship – bottom panel]-based measurements. Spatial and temporal windows are displayed in the left and right panels respectively.

Table 3. Error statistics of retrieved parameters

Parameter	Platform	*n*	Bias	RMSD (with bias)	RMSD (no bias)	*r* %
SST	DB	383	– 0.48	1.21	1.15	84
WS	MB	85	3.13	3.45	1.52	81
Q_a	AWS	254	1.78	2.54	1.81	60

10 m/s. High coefficient of correlation was obtained between satellite-derived WS and WS measured from stationary platforms such as MB and AWS. However, the correlation deteriorated for moving platforms like ship. WS measured from ocean platforms (MB and ship) was closer to the satellite values during daytime, while the land-based measurement from (AWS) indicated better correlation with satellite values during night hours. MSMR retrieval accuracy of SST and WS improved when validated with data collected over the tropical Indian Ocean. The accuracy, however, decreased for Q_a when compared with the achievable accuracy of WV from microwave channels. Each of the *in situ* sensors had its own inherent errors and varying accuracies as the sensors were not inter-calibrated. Therefore, inter-calibration must be an integral component of any satellite validation experiment.

1. *IRS-P4 Data User's Handbook*, Indian Remote Sensing Satellite–P4 (OCEANSAT-1), National Remote Sensing Agency, Department of Space, Govt. of India, Hyderabad, 1999, p. 74.
2. Cracknel, A. P., Remote sensing in meteorology. *Oceanogr. Hydrol*., 1981, 27–44.
3. Lipes, R. G. *et al.*, Seasat scanning multi-channel microwave radiometer: Results of the Gulf of Alaska workshop. *Science*, 1979, **204**, 1415.
4. Njoku, E., Stacey, J. M. and Frank, T. B., The Seasat scanning multi-channel microwave radiometer (SSMR): Instrument description and performance. *IEEE J. Ocean. Eng.*, 1980, **0E-5**, 100–115.
5. Smith, E., A user's guide to the NOAA Advanced Very High Resolution Radiometer Multichannel Sea Surface Temperature data set produced by the University of Miami/Rosentiel School of Marine and Atmospheric Science, Jet Propulsion Laboratory, Pasadena, 1992.
6. Wentz, F. J., Cardone, V. J. and Fedor, L. S., Intercomparison of wind speed inferred by the SASS, Altimeter and SMMR. *J. Geophys. Res*., 1982, **87**, 3378–3384.
7. Staelin, D. H., Kunzi, K. F., Petty John, R. L., Poon, R. K. L., Wilcox, R. W. and Waters, J. W., Remote sensing of atmospheric water vapor and liquid water with the Nimbus 5 microwave spectrometer. *J. Appl. Meteorol*., 1976, **15**, 1204–1214.
8. Schlussel, P., Schanz, L. and Englisch, G., Retrieval of latent heat flux and long wave irradiance at the sea surface from SSM/I and AVHRR measurements. *Adv. Space Res*., 1995, **16**, (10)107–(10)116.
9. Liu, W. T., Statistical relation between monthly mean precipitable water and surface level humidity over global oceans. *Mon. Weather Rev*., 1986, **114**, 1591–1602.
10. Ali, M. M., Validation of multi-frequency scanning microwave radiometer geophysical parameters data products. *PORSEC Proc.*, 2000, vol. I, pp. 182–191.
11. Wilheit, T. T., A review of applications of microwave radiometry to oceanography. *Boundary-Layer Meteorol*., 1978, **13**, 277–293.
12. Hsiung, J., Mean surface energy fluxes over the global ocean. *J. Geophys. Res*., 1986, **91**, 10,585–10,606.
13. Singh, R., Simon, B. and Joshi, P. C., A direct retrieval technique for near surface specific humidity and surface latent heat flux from Oceansat data. *PORSEC Proc*., 2002, vol. II, pp. 596–600.

ACKNOWLEDGEMENTS. We thank the Director, National Institute of Oceanography for the facilities and encouragement, and the Director, Space Applications Centre, Ahmedabad for providing funds to support this project. The National Remote Sensing Agency, Hyderabad supplied satellite data. We thank the Director, National Institute of Ocean Technology, Chennai for providing moored buoy data. We also thank Dr Satheesh Chandra Shenoi for providing drifting buoy data deployed over the tropical Indian Ocean during the period of validation, and Dr Ismail Koya, Science and Technology Department, Kavarathi, Lakshadweep Islands for surface met data from the AWS installed there as part of the validation experiment. This is NIO contribution no. 3916.

Received 30 April 2003; revised accepted 30 April 2004